processes

MDPI

Article

Preparation of Titanium Carbide by Carburisation of Titanium Dioxide

Tingting Lv [1,2,3], Fang Tian [1,2,3,4,*] and Tu Hu [1,2,3,*]

[1] Faculty of Metallurgical and Energy Engineering, Kunming University of Science and Technology, Kunming 650093, China; lv_tingting0123@163.com
[2] Yunnan Provincial Key Laboratory of Intensification Metallurgy, Kunming University of Science and Technology, Kunming 650093, China
[3] State Key Laboratory of Complex Nonferrous Metal Resources Clean Utilization, Kunming University of Science and Technology, Kunming 650093, China
[4] Shandong Research and Design Institute of Industrial Ceramics Co., Ltd., Zibo 255000, China
* Correspondence: tian_fang1110@126.com (F.T.); hutu_kust@126.com (T.H.)

Abstract: Titanium carbide has attracted widespread attention due to its excellent properties. This study investigates the process of carbon thermally reducing TiO_2 to prepare TiC through a combination of thermodynamic analysis and experiments. The effects of temperature, TiO_2/C molar ratio, and time on the phase transformation and morphology evolution of the products are investigated. The synthesis of titanium carbide involves the main reduction path of TiO_2–Magnéli–Ti_3O_5–Ti_2O_3–TiC_xO_{1-x}. With the increase in reaction temperature and TiC content, the microstructure transitions from a smooth disc-like structure to a loose and porous layered structure, while the particle size decreases significantly. The carburisation rate of the reduced product is more affected by temperature, according to chemical analysis. The carburisation rate increased from 18.37% to 36.09% for 2 h–10 h of holding time at 1400 °C, and from 51.43% to 77.57% for 2 h–10 h of holding time at 1500 °C. The quantification of the carburisation rate provides a valuable reference for the preparation of titanium carbide by TiO_2.

Keywords: carbothermic reduction; TiO_2; C; TiC; carburisation rate

Citation: Lv, T.; Tian, F.; Hu, T. Preparation of Titanium Carbide by Carburisation of Titanium Dioxide. *Processes* **2024**, *12*, 102. https://doi.org/10.3390/pr12010102

Academic Editor: Antonino Recca

Received: 21 November 2023
Revised: 22 December 2023
Accepted: 25 December 2023
Published: 1 January 2024

1. Introduction

TiO_2, which is an important titanium-containing material, is used to produce sponge titanium and other high-value titanium-containing products, including titanium carbide. Titanium carbide is a typical transition metal carbide with a high melting point, high hardness (28.5–32 GPa), excellent elastic modulus, good conductivity, low density, and good corrosion resistance [1–6]. It is widely applied in the fields of metal ceramics, mechanical manufacturing, and electrode materials [7–10]. Apart from that, TiC serves as an adsorbent for adsorbing gases, such as NH_3, CH_4, CO, etc., for environmental remediation due to its large specific surface area and rich active sites [11]. The broad application prospects of titanium carbide have attracted a large number of scholars to explore various synthetic methods for titanium carbide.

To avoid intermediate products and synthesize high-quality titanium carbide, Dunmead et al. employed direct carbothermal reduction by metallic titanium powder and carbon [12]. It costs a lot to use titanium metal as a raw material. Titanium tetrachloride can react with calcium carbide or methane to produce TiC [13–16]. Titanium tetrachloride is highly corrosive, so the corrosion resistance of the reaction vessel is crucial. Compared to titanium powder and titanium tetrachloride, titanium dioxide as a raw material is more popular. TiC can be formed by the reaction of solid carbon and titanium dioxide with a high temperature (1700–2000 °C) and long reaction time (10–20 h) [17,18]. The diffusion of carbon is the controlling step in the reaction. Hence, increasing the temperature and

time facilitates the formation of carbides [19]. In addition to solid carbon, hydrocarbon gases are alternative reducing agents. Professor Oleg Ostrovski has conducted research on the chemical reactions of Cr_2O_3, MnO, and CH_4. The results have shown that methane, as a carbonizing agent, can facilitate the formation of carbides at lower temperatures and shorter times compared to traditional carbon sources [20,21]. This discovery has opened up a new pathway for the carbothermic reduction of metal oxides. Zhang et al. showed that a mixture of methane and hydrogen can completely reduce TiO_2 to TiC_xO_y at 1350 °C for 8 h [22]. Methane is easily decomposed into carbon and hydrogen with increasing temperature, and carbon deposition causes the reaction to be hindered when the rate of methane decomposition is higher than the reaction [22–24]. The decomposition rate of methane cannot be determined, which makes it difficult to control the amount of carbon in the reduction process. In addition, both methane and hydrogen are highly flammable and explosive gases, so the equipment used for storage, transportation, and reaction processes must have high gas tightness requirements. The production cost of hydrogen is also high. Compared to gas reduction, solid carbon reduction is less hazardous and easier to control. Therefore, solid carbon is still dominant as a reducing agent in industrial production.

There have been many studies on the synthesis of carbides by the reduction of titanium oxides, but all of them are confined to the investigation of the reaction conditions and processes [22,23,25], and the degree of carbonisation of titanium oxides into titanium carbide has rarely been reported. Therefore, further research on the carbon thermal reduction of titanium oxides is necessary. The reaction process for the synthesis of titanium carbide was investigated by combining thermodynamic calculations and experiments. The evolutions in the phases and microstructure of the products are investigated by XRD and SEM. Finally, the ratio of carburisation is calculated based on the total titanium and titanium carbide content of the product obtained by chemical analysis, which directly reflects the synthesis of titanium carbide.

2. Materials and Methods

The pigment-grade TiO_2 and graphite powder are both analytical-grade reagents (99.9%, Aladdin Reagent Co., Ltd., Shanghai, China). Anhydrous ethanol is used as a dispersant (99.99%, Aladdin Reagent Co., Ltd., Shanghai, China). Argon gas is used as a protective gas (99.999%, Kunming Pengyida Gas Co., Ltd., Kunming, China). X-ray diffraction (XRD) of raw material is shown in Figure 1, which displays the diffraction peaks of rutile TiO_2. The scanning electron microscopy (SEM) of raw materials in Figure 1 shows that TiO_2 presents a smooth and dense disc-like structure. These disc-like particles are stacked and bonded to each other, meaning that TiO_2 is viscous and not easily dispersed.

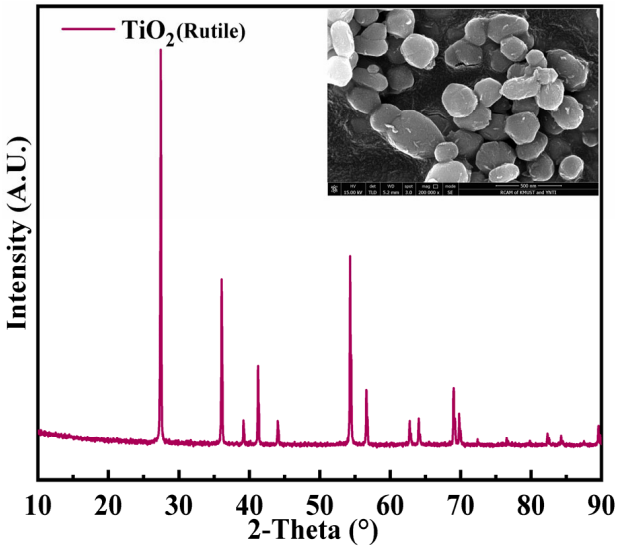

Figure 1. Raw material: TiO_2 (rutile).

Raw materials, TiO_2 and graphite, are mixed in a certain molar ratio. To prevent material stratification, anhydrous ethanol is added to the mixed powder as a dispersing agent, and the mixture is stirred in a magnetic stirrer to ensure uniform blending. Uniformly mixed material is then removed and dried in a drying oven at 120 °C for 6 h. Next, (3.0 ± 0.1) g of the mixture is removed and transferred to a pellet mould with a diameter of 15 mm. Subsequently, the mold is positioned onto a hydraulic press, applying a pressure of 2 MP to compact the powder into a sphere. Then, they are placed in a basket made of woven alloy wire as a substitute for a crucible. In addition, the basket is suspended in the temperature-controlled zone of the reaction furnace to maintain a constant temperature during the reduction process and adhere to the principle of controlling variables consistently. Argon gas does not participate in the reaction but serves as a protective gas. In addition to its role as a protective gas, argon can also be used to cool down the samples after the insulation time is completed. Argon is maintained at a constant flow rate of 300 sccm/min throughout the experiment.

The detection of the physical phase, micro-morphology, and elemental distribution of the products makes it possible to understand the course of the entire reaction process. The phase of the reduced product was determined using X-ray diffraction (XRD) with Cu Kα radiation. Scanning electron microscopy (SEM) was employed to observe the microscopic morphology of the samples. Microanalysis was performed using energy-dispersive spectroscopy (SEM/EDS) with an accelerating voltage of 10 kV. The product obtained from titanium oxide by carbothermal reduction is titanium oxycarbide rather than pure titanium carbide, which means that the degree of carbonisation of titanium oxide to titanium carbide needs to be obtained by calculation. Carburisation rate can directly reflect the synthesis of titanium carbide and be used as an important indicator for evaluating the degree of product carbonisation. A higher carburisation rate indicates higher amount of titanium carbide. Carburisation rate is the ratio of titanium carbonate (TiC) to total titanium (TTi) as in Equation (1) [26].

$$\eta = \frac{TiC}{TTi} \times 100\% \quad (1)$$

TiC is the amount of titanium carbide in the product, wt%; *TTi* is the amount of total titanium in the product, wt%; η is the carburisation rate of the product percentage.

3. Results

3.1. Thermodynamic Calculation

Thermodynamic analysis is an important tool for predicting the reduction conditions and pathways. In this study, thermodynamic analysis was conducted by the equilibrium and reaction modules of the Factsage 8.1 software, with a database provided by Cao et al. [27]. The results of the calculation are displayed in Figure 2. From the graph, it can be observed that synthesizing titanium carbide from titanium dioxide occurs stepwise. As the temperature increases, titanium dioxide is progressively reduced to lower titanium oxides until Ti_3O_5 is formed, followed by the appearance of TiC. Interestingly, the occurrence of carbide reaction is not only dependent on temperature but also closely related to the carbon content. When the molar ratio of TiO_2/C is 1:2 at 1400 °C, the final product consists of both Ti_3O_5 and TiC. There is a reserve of Ti_3O_5 in the product, and insufficient carbon causes incomplete carburisation. Increasing the amount of carbon, the molar ratio of TiO_2/C = 1:3, and titanium carbide was the only product at 1400 °C, indicating that Ti_3O_5 is completely carburised to TiC. Further increasing the molar ratio to 1:4 leads to the coexistence of TiC and residual carbon in the product. A molar ratio of 1:3 results in the complete carburisation of the titanium oxide to TiC, whereas a molar ratio of 1:4 has residual carbon, resulting in a waste of carbon. The thermodynamic analysis suggests that the molar ratio of TiO_2/C is 1:3 and a temperature of 1400 °C are favorable for synthesizing TiC.

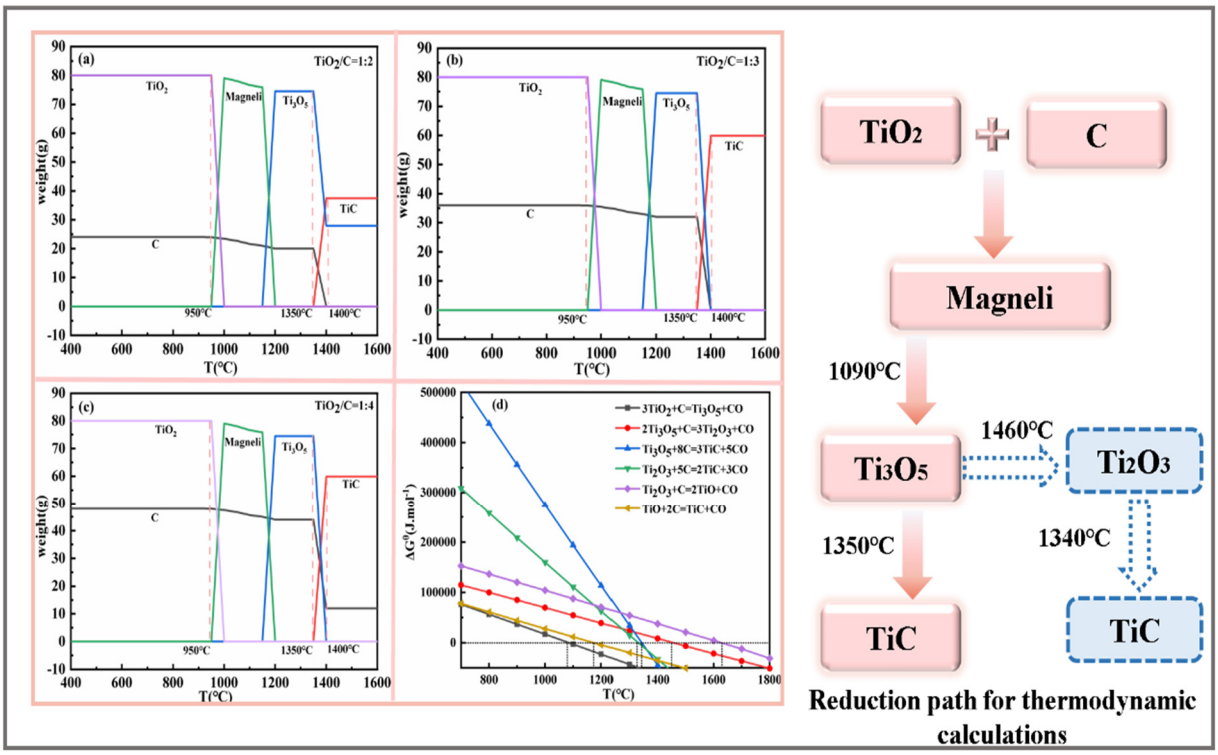

Figure 2. Thermodynamic calculation: (**a**) molar ratio TiO_2/C = 1:2; (**b**) molar ratio TiO_2/C = 1:3; (**c**) molar ratio TiO_2/C = 1:4; (**d**) Gibbs free energy of reaction.

Merely utilizing the equilibrium module is not sufficient for predicting the reduction pathway. The sequence of the reactions can be deduced based on the Gibbs free energy of the reactions. It is highlighted that all reactions have the potential to occur within the designated temperature range in Figure 2d. It is also demonstrated that TiO_2 is initially reduced to Ti_3O_5. The temperatures for the carbonation of Ti_3O_5 and Ti_2O_3 to TiC are very similar, as seen from the Gibbs free energies. However, in comparison to the reduction reaction, the carburisation of Ti_3O_5 is more likely to occur. The reduction of Ti_3O_5 to Ti_2O_3 requires a temperature of 1460 °C, while direct carburisation only requires 1350 °C, which leads to a preference for carburisation over the reduction of Ti_2O_3. This clarifies why the calculation results of the equilibrium module do not show Ti_2O_3. Combining the above thermodynamic calculations, including the physical phase transition and the Gibbs-free energy of the reaction, it is easy to obtain the pathway for the synthesis of TiC by the reaction of TiO_2 and C as TiO_2–Magnéli–Ti_3O_5–TiC (TiC_xO_{1-x}).

3.2. Effect of Temperature

Thermodynamic analysis results indicate that carbon and temperature are important factors for the preparation of titanium carbide. The influence of temperature on the reduction process is investigated with a molar ratio of TiO_2/C of 1:3 and a holding time of 10 h. The X-ray diffraction (XRD) results displayed in Figure 3 illustrate the outcomes of various reduction temperatures. Carbon and TiO_2 are a solid–solid reaction, and contact between the reactants and reaching the required temperature are prerequisites for the reaction to occur. The dominant phases are Ti_2O_3 and carbon, while a little of TiO_2 is present at 1300 °C, implying that TiO_2 is not completely reduced. A reduction reaction can occur, but the rate is very slow, leading to incomplete reduction. No carbide is detected at this temperature, meaning the carburising reaction has not yet started, or the carburising reaction is weak and the amount of carbide produced is too low to be detected. Raising the temperature to 1400 °C, signs of carbide are observed, suggesting that Ti_2O_3 is carburized to form carbides, but the carburization rate is slow. Thermodynamic calculations predict that complete carburisation into TiC is achievable at 1400 °C, but there is a discrepancy with

the experimental results, which is attributed to the impeded diffusion of gaseous products and the reduced contact area of titanium oxide with carbon as the reaction proceeds. The reduction of TiO_2 leads to pores hindering the contact between carbon and reactants and decreasing the reaction rate [28]. At 1500 °C, the predominant phase is TiC_xO_{1-x}, meaning that higher temperatures enhance the rate of carbide formation. Higher temperatures are an effective way to increase the rate of carburization. When the temperature increases from 1300 °C to 1500 °C, the diffraction peaks of titanium oxides decreases and the diffraction peaks of carbides are enhanced, indicating that there is a shift from a reduction-dominated reaction to a carbonation-dominated reaction in the TiO_2–C system. Additionally, the diffraction peak strength of carbon decreases sharply with a diffraction peak of carbide increases, signaling that a higher amount of carbon is required for carbide compared to reduction.

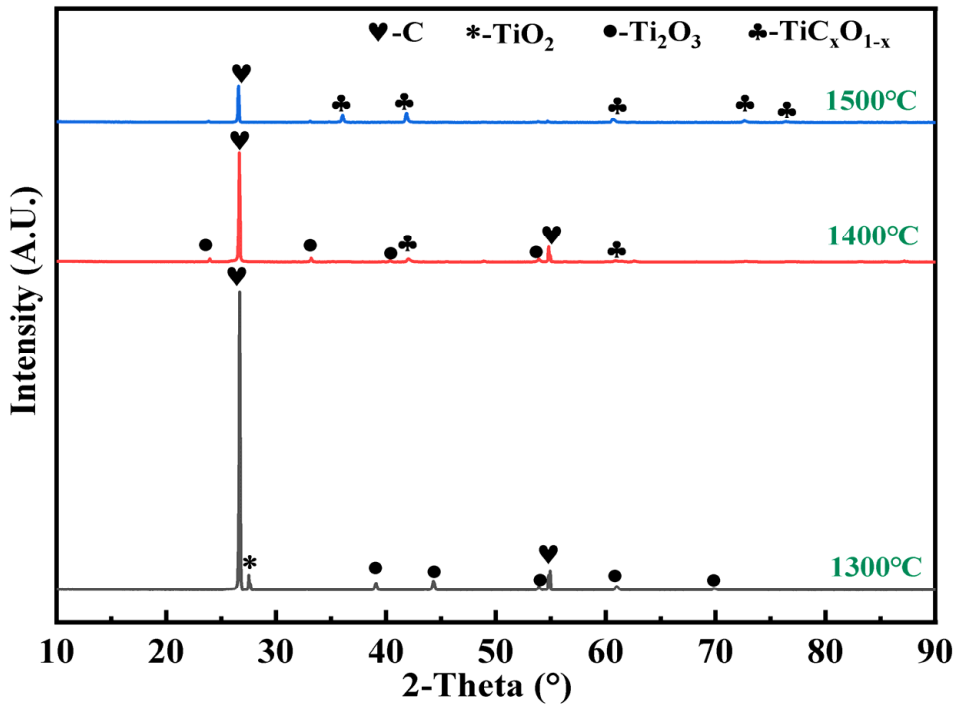

Figure 3. Phase evolution at different temperatures (molar ratio TiO_2/C = 1:3, holding time 10 h).

3.3. Carbon Content

The effects of carbon content were investigated at 1500 °C and 10 h of holding time. The evolution of phases is shown in Figure 4. When the molar ratio of TiO_2 to C is 1:1, the reduction products consist of Ti_2O_3, a little carbon, and carbides. The primary function of carbon is to reduce TiO_2 to low-valence titanium oxide. The desired TiC_xO_{1-x} phase appears at TiO_2/C = 1:1, indicating that the carbide reaction has started. Although the presence of carbides can be detected, the low intensity of the diffraction peaks shows that the amount of carbon is crucial for the formation of TiC_xO_{1-x}. Increasing the carbon content enhances the diffraction peaks of TiC_xO_{1-x}, while simultaneously decreasing the diffraction peaks of Ti_2O_3. This observation suggests that the reaction for carbide formation is intensified at the molar ratio of 1:2 TiO_2 to C. The characteristic peaks of TiC_xO_{1-x} dominate, leaving a few Ti_2O_3 phases at TiO_2/C = 1:3. Further increasing the molar ratio of TiO_2 to C does not result in any change apart from excess carbon, which leads to increased costs associated with subsequent carbon separation. When compared to other phases, the diffraction peaks of carbon exhibit a higher intensity at TiO_2/C = 1:4, a result that aligns with the findings of thermodynamic calculations. The appropriate amount of carbon is one of the key factors for synthesizing TiC_xO_{1-x}. In addition, carbon can be detected due to its high oxidation resistance and thermal stability [29]. Carbon does not readily oxidize

or decompose at high temperatures and remains relatively stable, making it an important reducing and carbonizing agent.

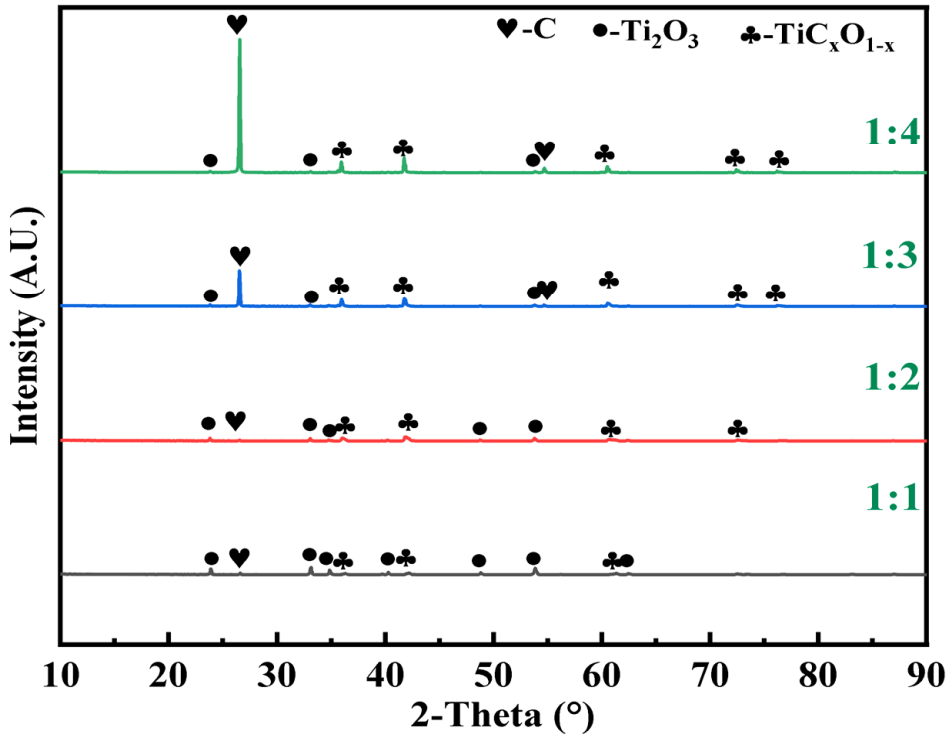

Figure 4. Phase evolution with different carbon content (at 1500 °C, holding time 10 h).

3.4. Holding Time

Figure 5 displays the reduction products at various holding times with a molar ratio of 1:3 at 1500 °C. After 2 h, high-valent titanium oxides are rapidly reduced to low-valent titanium oxides and carburisation occurs. The product is composed of carbon, Ti_2O_3, and carbide. That is, when the temperature and the amount of carbon are appropriate, the carburisation reaction occurs rapidly. Diffraction peaks of TiC_xO_{1-x} became stronger and the diffraction peaks of Ti_2O_3 decreased after 4 h, indicating that more and more oxides were transformed into carbide. At a holding time of 6 h, TiC_xO_{1-x} emerged as the predominant phase, demonstrating that carbide increases with prolonged holding time. At 8 h, the diffraction peak intensity of titanium oxide and carbon decreased. Continuing the extension of holding time to 10 h, the phase composition of the products remained unchanged and the peak intensities of carbon and Ti_2O_3 decreased, while the peak intensity of TiC_xO_{1-x} increased. After 12 h of holding, there was no significant change, meaning that there was no sense in extending the holding time. At 2 h–6 h, carbon diffraction peaks decreased sharply, the number of diffraction peaks for Ti_2O_3 decreased, and the diffraction peaks of carbide increased gradually, indicating that there was sufficient carbon around the oxide and that the rate of the carburisation reaction was fast. However, at 8 h–12 h, the product diffraction peaks show little change and the rate of the carburisation reaction decreases, which is attributed to the lower amount of carbon and its non-uniform distribution. Reduced contact between the carbon and the oxide causes the reaction to be more difficult. The reduction process can be described as TiO_2–Magnéli–Ti_3O_5–Ti_2O_3–TiC_xO_{1-x} based on our experimental findings. However, these results differ from the reduction process predicted by thermodynamic calculations, which will be discussed in the following sections.

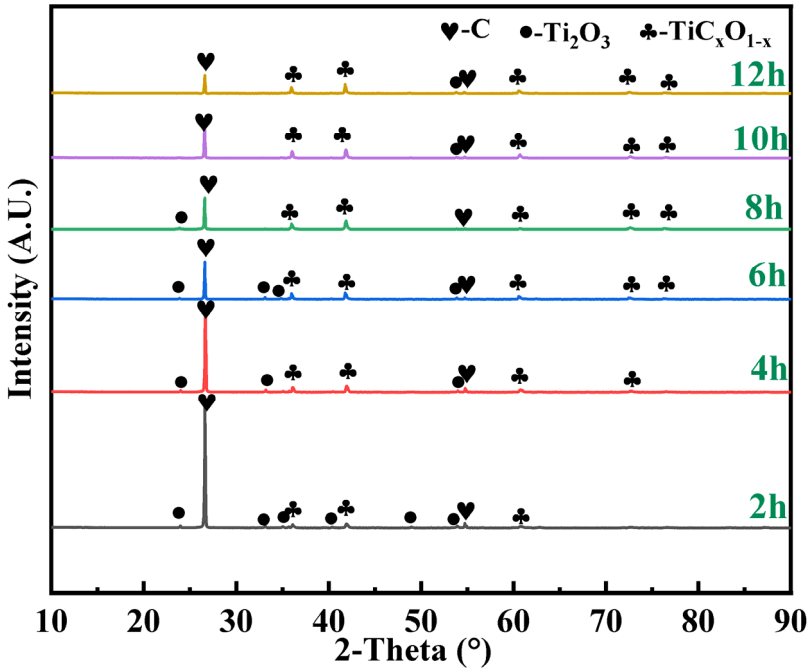

Figure 5. Phase evolution at different times (at 1500 °C, molar ratio TiO_2/C = 1:3).

3.5. Carburisation Rate

The content of total titanium and titanium carbide in the product was obtained based on chemical analysis as shown in Table 1. The amount of both titanium carbide and total titanium increased with increasing temperature and holding time, which demonstrated enhanced carburisation. Combined with Table 1 and Equation (1), the carburisation rate is calculated as shown in Figure 6, which increases with temperature and holding time. At 1400 °C, the carburisation reaction has occurred, and the rate of carburisation is relatively low. After a 2 h insulation period, the carburisation rate is measured to be 18.4%. Despite the potential benefits of prolonging the insulation time for carbide formation, even after a 10 h insulation period, the carburisation rate only reaches 36.1%. This suggests that there are still numerous titanium oxides remaining that have not undergone carburisation. At 1500 °C, the carburisation rate is 51.43% after 2 h. This finding strongly suggests that temperature plays a crucial role in influencing the carburisation reaction, and higher temperatures result in more vigorous carburisation reactions. By further extending the incubation time to 10 h, an impressive carburisation rate of 77.6% is achieved. In other words, at 1500 °C, a prolonged holding time is favourable to improve the degree of carburisation of titanium oxides. Interestingly, the carburisation rate does not uniformly increase as the incubation time is extended. The carburisation rate increases rapidly during the insulation period of 2 to 8 h, but afterwards, the rate of increase slows down. The intensification of the carbon gasification reaction leads to an increase in the partial pressure of CO with temperature rising. The gas fills the pores hindering direct contact between carbon and titanium oxide, which slows down the carburisation reaction. Additionally, the diffusion of carbon also serves as a factor influencing the carburisation reaction. The diffusion of unreacted carbon to regions in direct contact with titanium oxide is crucial for the continuation of the carburisation process. As the carburisation reaction progresses, the required time for carbon to diffuse to the target locations increases, resulting in a slower increase in the carburisation rate.

Table 1. Content of titanium carbide and total titanium (1400 °C and 1500 °C), holding time is 2–10 h.

Temperature (°C)	Time (h)	TiC (wt%)	TTi (wt%)
1400	2	11.02	48
1400	4	15.57	51
1400	6	20.74	52
1400	8	23.62	53
1400	10	23.91	53
1500	2	36	56
1500	4	50	61
1500	6	56	63
1500	8	62	65
1500	10	64	66

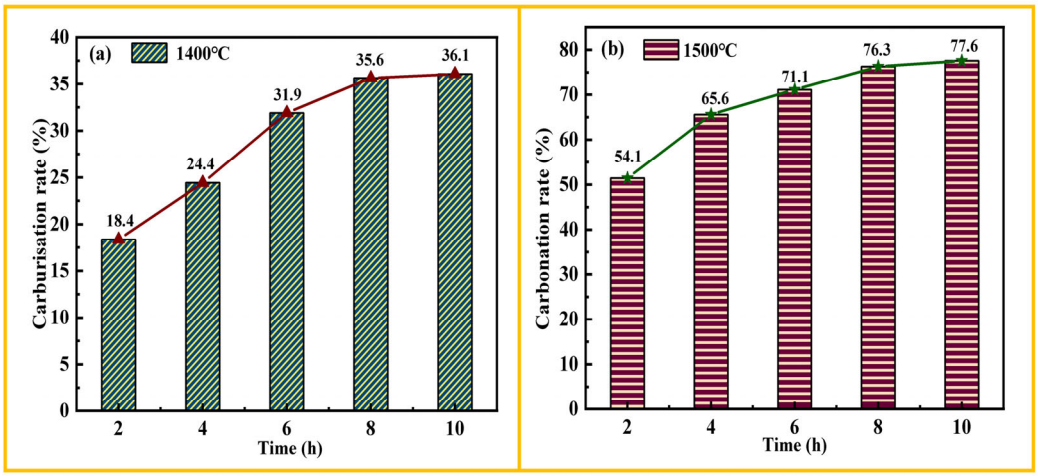

Figure 6. Variation of carburisation rate with temperature and time: (**a**) 1400 °C (molar ratio TiO_2/C = 1:3); (**b**) 1500 °C (molar ratio TiO_2/C = 1:3).

4. Discussion

4.1. Reduction Route

TiC_xO_{1-x} was prepared at a molar ratio of TiO_2/C = 1:3, at 1500 °C and 10 h. However, there are discrepancies between the thermodynamic calculations and experimental results regarding the path for synthesizing carbide. The presence of TiO_2, Magnéli, Ti_3O_5, and TiC, based on thermodynamic calculations, suggests that Ti_3O_5 is a precursor of carbide. Nevertheless, Ti_3O_5 was not detected in the experimental results, with the main phases being TiO_2, Ti_2O_3, and TiC_xO_{1-x}. Therefore, it can be inferred that the precursor for carbide is Ti_2O_3. The reason for the absence of Magnéli and Ti_3O_5 is that the rate of reduction from TiO_2 to Ti_3O_5 is very fast, and it is fully reduced under these experimental conditions. To explain the discrepancy between theoretical and experimental results, some clues can be drawn from the reaction equations. From the Reaction Equations (2)–(4), Ti_3O_5 directly carburizes into TiC, requiring eight moles of carbon. However, the pathway through Ti_3O_5–Ti_2O_3–TiC only requires 5.5 moles of carbon. Although the amount of carbon is sufficient to generate titanium carbide, during the reduction process, a portion of the carbon that comes into contact with the titanium oxide is consumed. As a result, the carbon content around the titanium oxide is reduced, causing Ti_3O_5 to be preferentially reduced rather than directly carburized. Koc and Folmer proposed that there are two pathways for the carbon thermal reduction of titanium oxide. When there is an excess of carbon and CO, Ti_3O_5 directly carburizes into carbide. However, if there is a deficiency of carbon and CO, it first undergoes a reduction to Ti_2O_3 and then carburizes into carbide [17]. In addition, the crystal structure is also one of the important factors influencing carburisation reduction. TiO_2 has a tetragonal crystal structure, Ti_3O_5 has a monoclinic crystal structure, Ti_2O_3 has a hexagonal crystal structure, and TiC has a cubic crystal structure. The reaction is

related to the crystal structure of the material, according to Welham [25]. When oxygen in the reactants is removed, the product undergoes minor rearrangement, resulting in an increase in symmetry. This increase in symmetry facilitates the subsequent formation of the cubic phase. The reduction of Ti_3O_5 to TiC may be limited by crystallographic constraints. It is more advantageous in terms of kinetics to conduct the carburization process using the intermediate phase Ti_2O_3, which possesses symmetry. The process of synthesising carbide in this work is shown in Figure 7. Firstly, there is a reduction stage, where TiO_2 is reduced until Ti_2O_3. Then, there is a carburisation stage. Ti_2O_3 undergoes a carburisation reaction to produce carbide. Based on the above analysis, it is suggested that the reduction pathway for carbon thermal reduction of titanium oxide in this experiment is TiO_2–Magnéli–Ti_3O_5–Ti_2O_3–TiC_xO_{1-x}.

$$Ti_3O_5 + 0.5C = 1.5Ti_2O_3 + CO \quad (2)$$

$$Ti_3O_5 + 8C = 3TiC + 5CO \quad (3)$$

$$Ti_2O_3 + 5C = 2TiC + 3CO \quad (4)$$

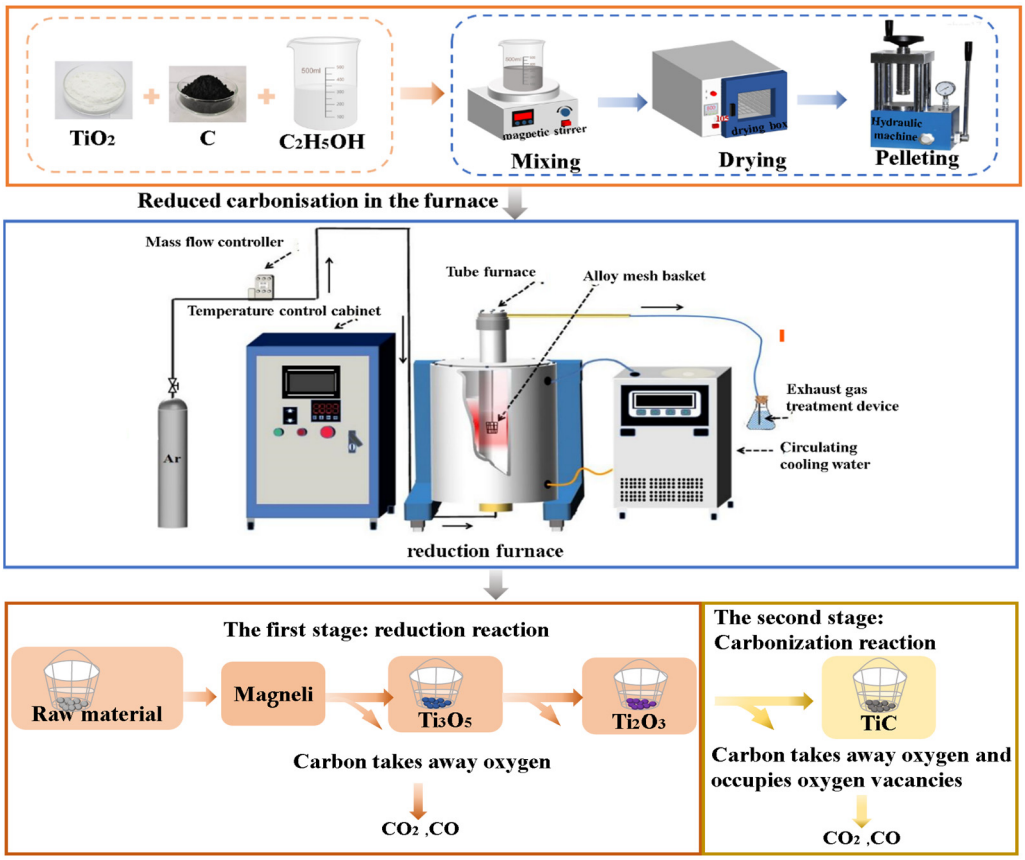

Figure 7. Carbothermal reduction process of titanium oxides.

4.2. Micro-Morphology

To facilitate the observation of changes in the morphology of the products, the reduced material was ground into a powdered form. Figure 8a,b show the micrographs of the raw material, while the TiO_2 surface is smooth and dense, presenting a disc-shaped structure. At 1300 °C, the surface of the samples starts to become rough, while the microstructure still retains the disc-shaped structure of the raw material. Upon further magnification, as shown in Figure 8d, the surface of the product exhibits a number of gas pores, which are caused by the release of CO during reduction. At this temperature, the main process occurring is the reduction of titanium oxides. The high-valence titanium oxides lose some oxygen and

transform into low-valence titanium oxides. The reduction reaction cannot alter the original microstructure of the reactants; it only results in the generation of a rough and porous surface through the release of gas. When continuing to rise the temperature to 1400 °C, the samples completely deviate from the disc-shaped dense structure and exhibit a loose surface state. Titanium oxide undergoes carbide formation, which completely changes the original microstructure of the material at 1400 °C. As shown in Figure 8f, the surface of the product becomes porous and exhibits a layered structure. However, at this temperature, the carburisation rate is not high and there still exists a significant portion of densely structured titanium oxide. After grinding, the particle size of the product changes minimally. At 1500 °C, Figure 8g indicates that not only does the surface of the product become porous, but the particle size also decreases dramatically, which is attributable to the intensified carburisation reaction. The product, TiC_xO_{1-x}, exhibits a porous structure, and the particle size decreases after grinding. In other words, at this point, carbides become the main phase. By further increasing the magnification, it can be observed that the sample exhibits a layered structure, indicating that carbides grow layer by layer [30]. Figure 9 presents the Energy Dispersive X-ray Spectroscopy (EDS) results for different temperatures. EDS results show the elemental composition, and the product consists of three elements: Ti, C, and O. The differences in temperature result in variations in the elemental proportions. At 1300 °C, a small amount of carbon is distributed at the edges of the particles, while the denser regions of the product lack carbon distribution. The distribution of carbon elements reflects the locations of the carbides, showing that only a small amount of titanium oxide undergoes carbide formation. Furthermore, the atomic proportion of oxygen, which is 50.9%, further confirms that the primary constituent in the product is titanium oxide. At a temperature of 1400 °C, the particles exhibit a layered structure on their surface. The distribution of carbon elements throughout the entire particle indicates that the carburisation reaction is enhanced as the temperature increases. Simultaneously, there is a decrease in the proportion of oxygen atoms, due to a gradual transformation of oxides into carbides. At 1500 °C, three elements are evenly distributed. Firstly, the oxygen in the titanium oxide is removed by the carbon in the form of gas. After the reduction reaction is mostly completed, carbon slowly diffuses towards the edges of the titanium oxide, depleting oxygen and infiltrating into oxygen vacancies to form titanium oxycarbide. With the progress of the carburisation reaction, the oxygen in titanium oxycarbide gradually decreases, and the corresponding amount of titanium carbide increases. The rate of carbide formation is primarily determined by the diffusion of carbon. In addition, higher temperatures promote carbon diffusion, thereby facilitating the formation of carbides.

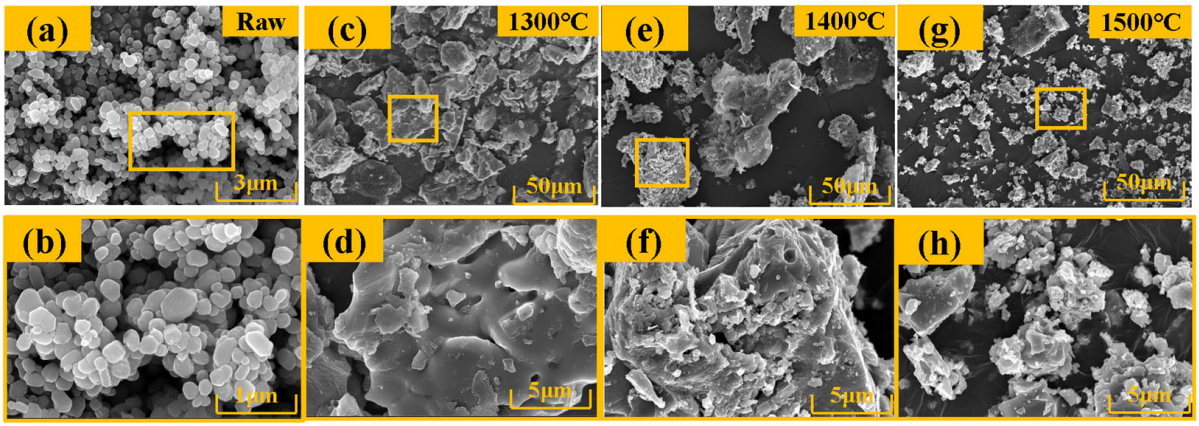

Figure 8. SEM images of holding at different temperatures for 10 h (**a**,**b**), Raw (**c**,**d**), 1300 °C (**e**,**f**), 1400 °C (**g**,**h**), 1500 °C.

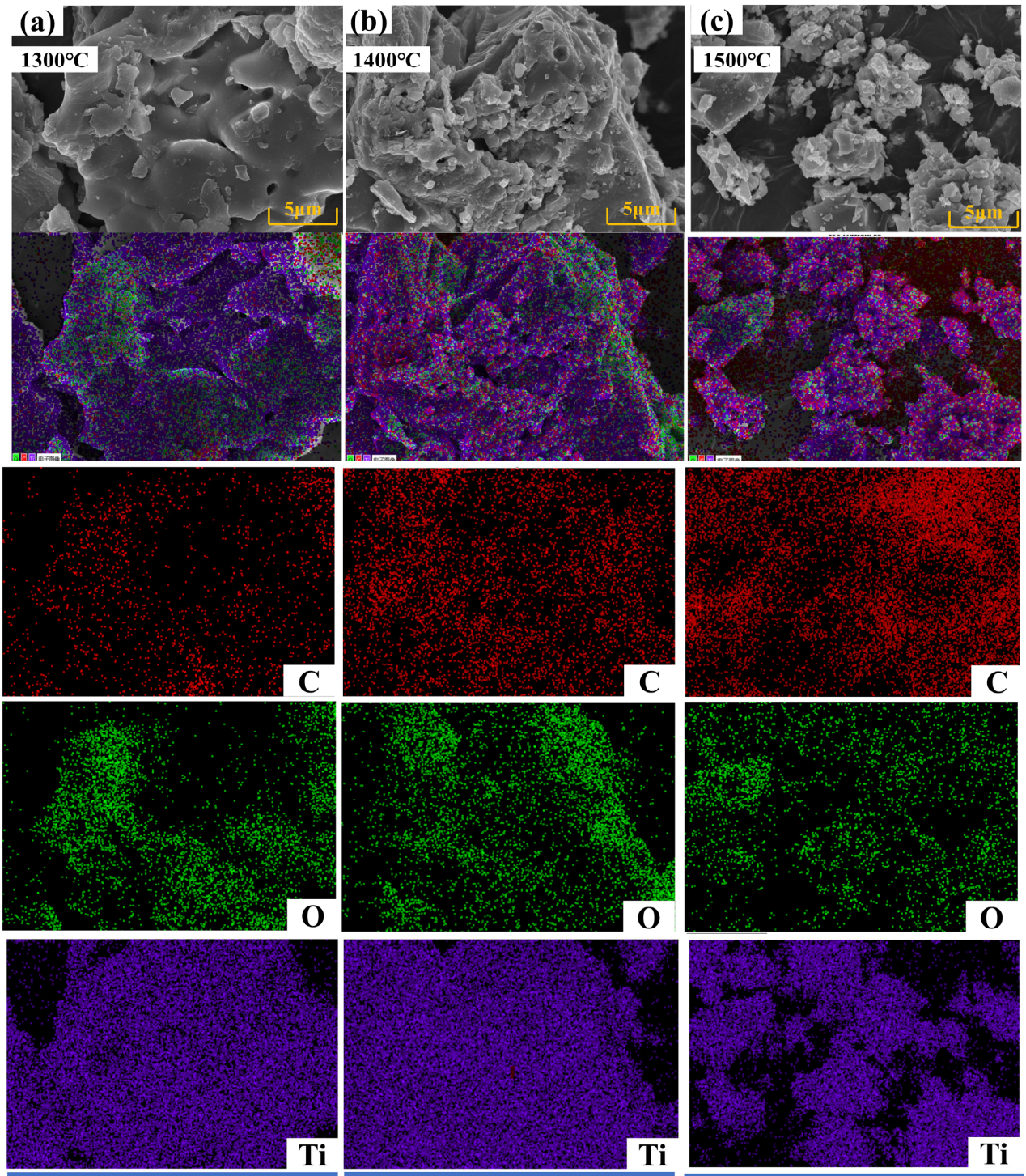

EDS analysis results	
Element	Atomic percentage
C	19
O	50.9
Ti	30.1
total	100

EDS analysis results	
Element	Atomic percentage
C	38.2
O	36.5
Ti	25.2
total	100

EDS analysis results	
Element	Atomic percentage
C	66.7
O	16.1
Ti	17.2
total	100

Figure 9. EDS results at different temperatures (molar ratio TiO_2/C = 1:3, holding time 10 h): (**a**) 1300 °C; (**b**) 1400 °C; (**c**) 1500 °C.

5. Conclusions

This study combines thermodynamics and experiments to investigate the process of preparing titanium carbide through the thermal reduction of TiO_2 and carbon (C). The following conclusions have been obtained:

1. The temperature, carbon content, and time are three important factors in the preparation of TiC_xO_{1-x}. Increasing the temperature provides heat for the reaction and promotes the diffusion of carbon into the surrounding titanium oxide, triggering the reaction. The appropriate carbon content is crucial for the preparation of carbides. A lower amount of carbon content yields only a small quantity of carbides, whereas an excessive carbon content results in a surplus of carbon and subsequently increased costs for separation. In addition, TiC_xO_{1-x} was prepared with a molar ratio of TiO_2/C = 1:3 at a temperature of 1500 °C for a duration of 10 h.
2. The intermediate phases Magnéli and Ti_3O_5 were not detected; they were attributed to the fast reduction rate of TiO_2 to Ti_2O_3, which does not mean that Magnéli and Ti_3O_5 were not produced during the reaction, and the titanium oxides were reduced stepwise. All of TiO_2 was reduced to Ti_2O_3, suggesting that the reduction ended and was followed by the carburisation of Ti_2O_3. In addition, the synthesis of titanium carbide involves the main reduction path: TiO_2–Magnéli–Ti_3O_5–Ti_2O_3–TiC_xO_{1-x}.
3. As the temperature rises from 1300 °C to 1500 °C, the amount of carbide increases. The microscopic morphology of the material gradually deviates from the original smooth and dense cake-like structure, which becomes rough and porous. After the abundant formation of carbides, the material displays a porous layered structure of carbides, which is completely separate from the original structure.
4. Temperature has a greater effect on the carburisation ratio compared to time. At a temperature of 1400 °C, with a holding time ranging from 2 h to 10 h, the carburisation ratio increases from 18.37% to 36.09%. At 1500 °C, the carburisation ratio increases from 51.43% to 77.57%. Overall, increasing the temperature and time favours the generation of titanium carbide.

Author Contributions: Conceptualization, T.H.; methodology, T.H.; formal analysis, T.L.; writing—original draft preparation, T.L. and F.T.; writing—review and editing, T.L.; funding acquisition, T.H. All authors have read and agreed to the published version of the manuscript.

Funding: This work was supported by the National Nature Science Foundation of China (U1902217), Yunnan Provincial Science and Technology Talents Program (202005AC160033), and Yunnan Ten Thousand Talents Plan Young and Elite Talents Project (YNWRQNBJ-2019-222).

Data Availability Statement: Data is available through the authors.

Conflicts of Interest: Fang Tian was employed by the company Shandong Research and Design Institute of Industrial Ceramics Co., Ltd. The remaining authors declare that the research was conducted in the absence of any commercial or financial relationships that could be construed as a potential conflict of interest.

References

1. Mao, J.J.; Li, S.S.; Zhang, Y.X.; Zhu, X.L.; Yang, Z.X. The stability of TiC surfaces in the environment with various carbon chemical potential and surface defects. *Appl. Surf. Sci.* **2016**, *386*, 202–209. [CrossRef]
2. Wang, Z.; Lin, T.; He, X.B.; Shao, H.B.; Tang, B.; Qu, X.H. Fabrication and properties of the TiC reinforced high-strength steel matrix composite. *Int. J. Refract. Met. Hard Mater.* **2016**, *58*, 14–21. [CrossRef]
3. Miao, S.; Xie, Z.M.; Zhang, T.; Wang, X.P.; Fang, Q.F.; Liu, C.S.; Luo, G.N.; Liu, X. Mechanical properties and thermal stability of rolled W-0.5 wt% TiC alloys. *Mater. Sci. Eng. A* **2016**, *671*, 87–95. [CrossRef]
4. Yoshioka, S.; Boatemaa, L.; Zwaag, S.V.D.; Nokao, W.; Sloof, W.G. On the use of TiC as high-temperature healing particles in alumina based composites. *J. Eur. Ceram. Soc.* **2016**, *36*, 4155–4162. [CrossRef]
5. Zhao, X.B.; Zhou, Y.G.; Liu, S.; Zhou, Y.F.; Zhao, C.C.; Wang, C.X.; Yang, Q.X. Investigation on WC/TiC interface relationship in wear-resistant coating by first-principles. *Surf. Coat. Technol.* **2016**, *305*, 200–207. [CrossRef]
6. CSahoo, K.; Soni, L.; Masanta, M. Evaluation of microstructure and mechanical properties of TiC/TiC-steel composite coating produced by gas tungsten arc (GTA) coating process. *Surf. Coat. Technol.* **2016**, *307*, 17–27. [CrossRef]

7. Ding, L.; Xiang, D.P.; Pan, Y.L.; Zhang, T.M.; Wu, Z.Y. In situ synthesis of TiC cermet by spark plasma reaction sintering. *J. Alloys Compd.* **2016**, *661*, 136–140. [CrossRef]
8. Acharya, S.; Debata, M.; Acharya, T.S.; Acharya, P.P.; Singh, S.K. Influence of nickel boride addition on sintering behaviour and mechanical properties of TiC-Ni based cermets. *J. Alloys Compd.* **2016**, *685*, 905–912. [CrossRef]
9. Oláh, N.; Fogarassy, Z.; Sulyok, A.; Szívós, J.; Csanádi, T.; Balázsi, K. Ceramic TiC/C protective nanocomposite coatings: Structure and composition versus mechanical properties and tribology. *Ceram. Int.* **2016**, *42*, 12215–12220. [CrossRef]
10. Zhang, Z.Q.; Yang, F.; Zhang, T.G.; Zhang, H.W.; Zhang, D.L. Research Progress of Laser Cladding Titanium Carbide Reinforced Titanium-based Composite Coating. *Surf. Technol.* **2020**, *49*, 138. [CrossRef]
11. Wu, Y.; Li, X.M.; Zhao, H.; Yao, F.B.; Cao, J.; Chen, Z.; Huang, X.D.; Wang, D.B.; Yang, Q. Recent advances in transition metal carbides and nitrides (MXenes): Characteristics, environmental remediation and challenges. *Chem. Eng. J.* **2021**, *418*, 129296. [CrossRef]
12. Dunmead, S.; Munir, Z.A.; Holt, J.B. Temperature Profile Analysis in Combustion Synthesis: II, Experimental Observations. *J. Am. Ceram. Soc.* **1992**, *75*, 180–188. [CrossRef]
13. Feng, X.; Bai, Y.J.; Lü, B.; Wang, C.G.; Liu, Y.X.; Geng, G.L.; Li, L. Easy synthesis of TiC nanocrystallite. *J. Cryst. Growth* **2004**, *264*, 316–319. [CrossRef]
14. Feng, X.; Bai, Y.J.; Lü, B.; Wang, C.G.; Liu, Y.X.; Geng, G.L.; Li, L. Low temperature induced synthesis of TiN nanocrystals. *Inorg. Chem.* **2004**, *43*, 3558–3560. [CrossRef] [PubMed]
15. Xiang, M.Q.; Song, M.; Zhu, Q.S.; Hu, C.Q.; Yang, Y.F.; Lv, P.P.; Zhao, H.D.; Yun, F. Facile synthesis of high-melting point spherical TiC and TiN powders at low temperature. *J. Am. Ceram. Soc.* **2019**, *103*, 889–898. [CrossRef]
16. Alexandrescu, R.; Borsella, E.; Bottl, S.; Cesile, M.C.; Martelli, S.; Giorgi, R.; Turtu, S. Synthesis of TiC and SiC/TiC nanocrystalline powders by gas-phase laser-induced reaction. *J. Mater. Sci.* **1997**, *32*, 5629–5635. [CrossRef]
17. Koc, R.; Folmer, J.S. Carbothermal synthesis of titanium carbide using ultrafine titania powders. *J. Mater. Sci.* **1997**, *32*, 3101–3111. [CrossRef]
18. Ali, M.; Basu, P. Mechanochemical synthesis of nano-structured TiC from TiO_2 powders. *J. Alloys Compd.* **2010**, *500*, 220–223. [CrossRef]
19. Welham, N.J.; Willis, P.E. Formation of TiN/TiC-Fe composites from ilmenite ($FeTiO_3$) concentrate. *Metall. Mater. Trans. B* **1998**, *29*, 1077–1083. [CrossRef]
20. Anacleto, N.; Ostrovski, O.; Ganguly, S. Reduction of Manganese Ores by Methane-containing Gas. *Trans. Iron Steel Inst. Jpn.* **2004**, *44*, 1615–1622. [CrossRef]
21. Anacleto, N.; Ostrovski, O. Solid-state reduction of chromium oxide by methane-containing gas. *Metall. Mater. Trans. B* **2004**, *35*, 609–615. [CrossRef]
22. Zhang, R.; Liu, D.; Fan, G.Q.; Sun, H.B.; Dang, J. Thermodynamic and experimental study on the reduction and carburisation of TiO_2 through gas-solid reaction. *Int. J. Energy Res.* **2019**, *43*, 4551. [CrossRef]
23. Fan, G.Q.; Hou, Y.L.; Huang, D.J.; Dang, J.; Zhang, R.; Xiang, J.Y.; Lv, X.W.; Ding, X.M. Synthesis of Ti(C, N, O) ceramic from rutile at low temperature by CH_4-H_2-N_2 gas mixture. *Int. J. Refract. Met. Hard Mater.* **2021**, *101*, 105659. [CrossRef]
24. Zhang, G.Q.; Ostrovski, O. Reduction of titania by methane-hydrogen-argon gas mixture. *Metall. Mater. Trans. B* **2000**, *31*, 129–139. [CrossRef]
25. Welham, N.J.; Williams, J.S. Carbothermic reduction of llmenite ($FeTiO_3$) and rutile (TiO_2). *Metall. Mater. Trans. B* **1999**, *30*, 1075–1081. [CrossRef]
26. Qing, J. Fundamental Study on Carburisation and Nitridation of Vanadium-Titanium Magnetite in the Process of Coal-Based Direct Reduction Followed by Magnetic Separation. Ph.D. Thesis, Chongqing University, Chongqing, China, 2020.
27. Cao, Z.M.; Xie, W.; Jung, I.H.; Du, G.W.; Qiao, Z.Y. Critical evaluation and thermodynamic optimization of the Ti-C-O system and its applications to Carbothermic TiO_2 reduction process. *Metall. Mater. Trans. B* **2015**, *46*, 1782–1801. [CrossRef]
28. Wang, K.F.; Sun, G.D.; Wu, Y.D.; Zhang, G.H. Fabrication of ultrafine and high-purity tungsten carbide powders via a carbothermic reduction–carburization process. *J. Alloys Compd.* **2023**, *784*, 362–369. [CrossRef]
29. Subasinghe, H.C.S.; Ratnayake, A.S. Effect of different carbon sources on the conversion of ilmenite into synthetic rutile via ball milling induced carbothermic reduction. *J. Alloys Compd.* **2023**, *954*, 170086. [CrossRef]
30. Long, W.; Gao, F.; Wang, D. Forming thermodynamics, structure, and electrical conductivity of TiCxOy compounds fabricated through the carbothermal reduction process. *J. Alloys Compd.* **2022**, *892*, 16220. [CrossRef]